Journal of Ceramic Processing Research. Vol. 18, No. 3, pp. 183~187 (2017)

J O U R N A L O F
Ceramic Processing Research

Characteristics of Y_2O_3 transparent ceramics rapidly processed using spark plasma sintering

Cheol Woo Park, Jung Hun Lee, Suk Hyun Kang, Jae Hwa Park, Hyun Mi Kim, Hyo Sang Kang, Hee Ae Lee, Joo Hyung Lee and Kwang Bo Shim*

Division of Advanced Materials Science and Engineering, Hanyang University, Seoul 04763, Korea

Commercially available Y_2O_3 powder was subjected to size and shape control followed by carrying out densification for 5 min at relatively lower temperatures (1400-1700 °C) using a spark plasma sintering (SPS) system to examine the optimum sintering conditions. The results showed that the specimen sintered at 1600 °C for 5 min while being pressurized at 30 MPa exhibited the highest sintering density (98.97%) and demonstrated the best transmittance performance. The annealing treatment of samples at oxygen atmosphere was very effective to increase their transmittance. The increased transmittance could be attributed to the decrease in oxygen vacancy and the removal of surplus carbon. Samples exhibiting superior mechanical properties and a high transmittance of 82.15% (i.e., 99% of the theoretical value) at a wavelength of 2000 mm were obtained.

Key words: Y_2O_3 Transparent ceramics, Spark plasma sintering, Densification, Microstructure.

Introduction

Transparent Y_2O_3 (yittria) ceramics have been extensively studied as a promising material for refractory and optical applications owing to their high corrosion resistance, thermal stability, and outstanding transparency over a wide range of wavelength [1, 2]. These ceramics have been usually produced using different sintering techniques such as hot pressing, hot isostatic pressing (HIP), and pressureless sintering; however, these techniques require extremely high sintering temperatures and the use of sintering aids. In spark plasma sintering (SPS), a pulsed direct current (PDC) passes through the powder to be sintered for accomplishing sintering at high-temperatures spark plasma occurring between the particles and the joule heat from the current passing through the powder-containing graphite molds [3, 4]. In this technique, the temperature can be increased from low to high values (> 2000 °C) within a short time. This facilitates the formation of necks between powder particles and cleans the surfaces of the crystallites. As compared to the conventional sintering methods, full sintering can be achieved at an extremely short time at low temperatures owing to the thermal diffusion and electric field diffusion effects [5, 6]. These merits have continued to encourage studies on the SPS-based production of transparent ceramics [7]. However, the SPS process requires a carbon-rich atmosphere and the use of graphite dies, which are used as a heater, and this might result in the production of carbon. Consequently, materials produced using SPS contain high levels of carbon, thereby potentially damaging the optical transparency [8]. Hence, it is crucial to implement carbon-removal processes based on annealing in the production of transparent ceramics via SPS for protecting the ceramic products against carbon contamination and increasing their transmittance.

In this study, we used SPS to produce transparent Y_2O_3 ceramics in a short time at lower temperatures without using a sintering agent. The study reveals the optimal sintering conditions by analyzing the relative density with respect to sintering temperatures as well as the microstructures and mechanical properties of the samples. Furthermore, annealing was carried out in oxygen atmosphere, and the optical properties of the specimen were investigated.

Experiment

Powder preparation and SPS sintering

High-purity, commercially available Y_2O_3 powder (99.99% pure; 150 nm; Cenotec, Korea) was used as the starting material. The Y_2O_3 powder was subjected to ball milling for 24 hrs at a weight ratio of 1 : 10 against zirconia balls of 1.5 mm in diameter. The powder was placed in an oven and dried at 60 °C for 2 days. It was then heated inside a box furnace for 30 min at 1000 °C with a heating rate of 10 °C/min. The heat-treated powder consists of relatively uniform, spherical grains of approximately 50-300 nm in diameter.

*Corresponding author:
Tel : +82-2-2220-0501
Fax: +82-2-2291-7395
E-mail: kbshim@hanyang.ac.kr

The prepared powder was inserted into a graphite die of 15 mm in internal diameter with its interior wrapped around in a graphite foil. Sintering of the powder was then carried out using an SPS system (Sumitomo Coal Mining, S-515S, Japan) at 1400-1700 ºC at 10 Pa (vacuum) and 30 MPa (axial pressurization). During sintering, the specimen was heated from ambient temperature to the final sintering temperature (max. 1700 ºC) with a rate of 100 ºC/min and held at the desired temperature for 5 min. The pressure during the process was maintained to be 30 MPa. Upon completion of sintering, pressure was released and the current was shut down. The sintered specimen, 15 mm in diameter and 1 mm in thickness, was then subjected to annealing in a box furnace in oxygen atmosphere for 4 hrs at 1100 ºC at the rate of 10 ºC/min. Both the surfaces of the specimen were ground for evaluating the microstructural and optical properties followed by polishing the surfaces using a 1 μm diamond paste.

Characterization

The morphology of the powder, average grain size of the specimens as well as the fractured surfaces of the sintered specimens were examined using a field emission-scanning electron microscope (FE-SEM, NOVA Nano SEM 450, FEI, Czech Republic) at acceleration voltages of 5-15 kV. The relative density of the specimens was measured using the Archimedes law. Before and after annealing, the in-line transmittance of the specimens was measured in the wavelength range of 300-2000 nm using a UV-Vis-NIR spectrophotometer (Lambda 950, Perkin-Elmer, America). The hardness of the specimens was calculated using a digital hardness tester (FV-700e, Future-Tech Co. Ltd, Japan) to obtain the average value from 15 indentation impressions.

Results and Discussion

Fig. 1 shows the photographs of the Y_2O_3 ceramic specimens sintered for 5 min using SPS at 1400-1700 ºC and 30 MPa. As the sintering temperature of the samples increases, the letters on the back of the specimen in the photographs can be seen with a greater clarity, indicating that the highest transparency is achieved at 1600 ºC and the transparency decreases at 1700 ºC. The transparency of the sintered specimens is closely related to their sintering density. Moreover, the transparency is affected with carbon diffusion occurring into the specimen, which is characteristic of SPS [8]. Fig. 2 provides the relative density and average grain size of the sintered specimens. With an increase in the sintering temperatures, the sintering density gradually increases and reaches the maximum value at 1600 ºC (1400 ºC, 98.85%; 1500 ºC, 98.859%; 1600 ºC, 98.966%). The sintering density decreases at temperatures higher than 1600 ºC (1700 ºC, 98.78%). Fig. 2 shows the SEM image of the surface of the specimen sintered at 1600 ºC and subjected to surface

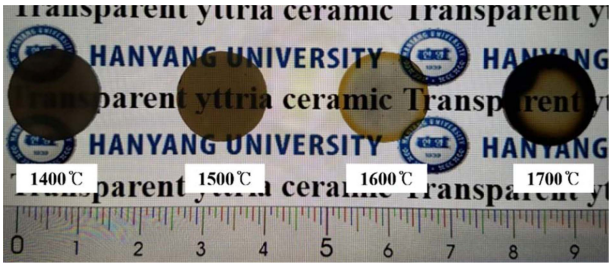

Fig. 1. Photograph of the Y_2O_3 specimens sintered at different temperatures.

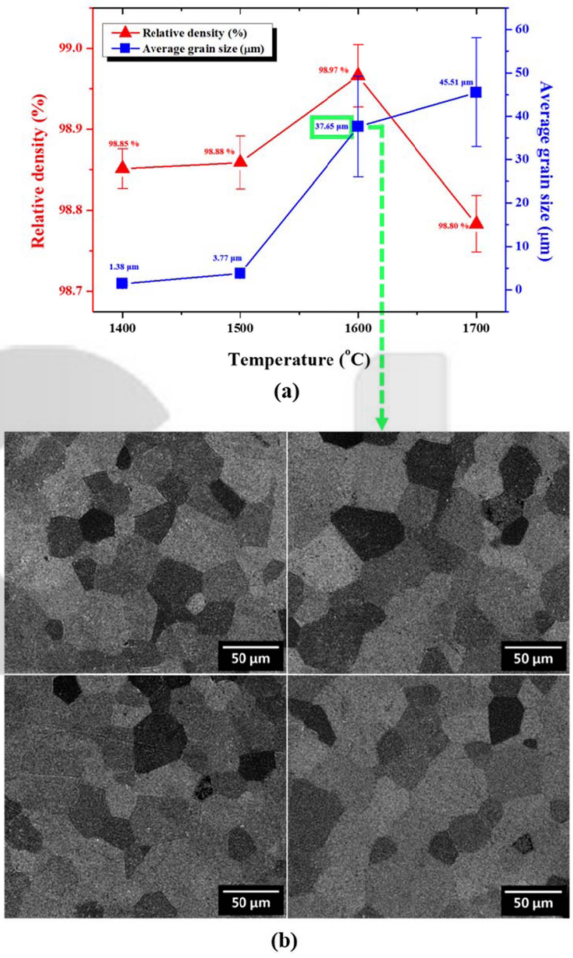

Fig. 2. (a) Variation in the relative density and average grain size with respect to the SPS temperature. (b) FE-SEM images of the thermal etched surfaces of Y_2O_3 ceramics sintered at 1600 ºC.

grinding and thermal etching at 1200 ºC. The formation of extremely dense, uniform microstructure with no intergranular or intragranular micropores suggests the occurrence of quick sintering followed by densification, thereby suppressing the normal grain growth. The average grain size of the specimens sintered at 1600 ºC was measured to be ~37.6 μm.

Fig. 3 shows the FE-SEM images of fractured surfaces of the specimens sintered using SPS at different temperatures. The surfaces exhibit a microstructure with

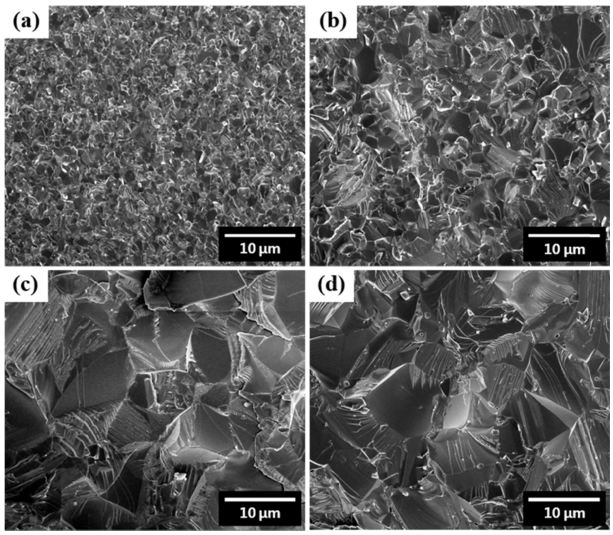

Fig. 3. FE-SEM images of the fractured surfaces of Y_2O_3 sintered at (a) 1400 ºC, (b) 1500 ºC, (c) 1600 ºC, and (d) 1700°C under a pressure of 30 MPa for 5 min.

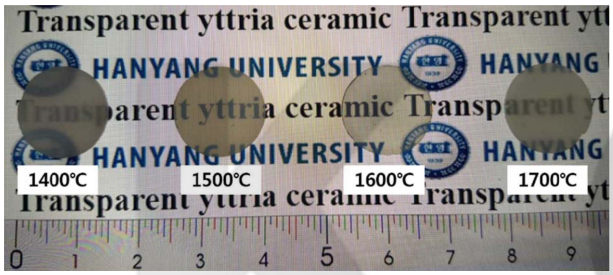

Fig. 4. Photographs of the as-annealed Y_2O_3 ceramics.

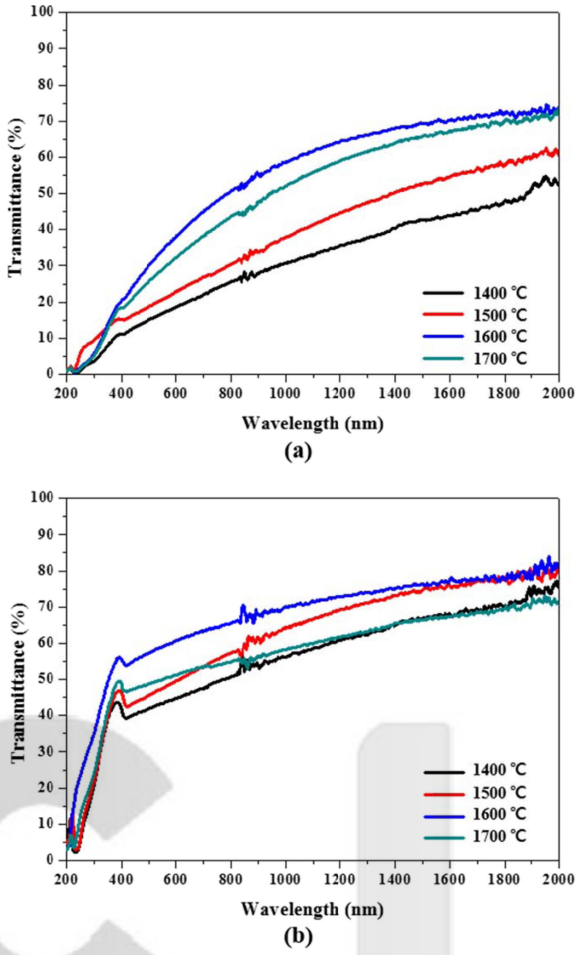

Fig. 5. Transmittance spectrum of the (a) as-sintered and (b) as-annealed samples treated at 1400-1700 ºC under a pressure of 30 MPa.

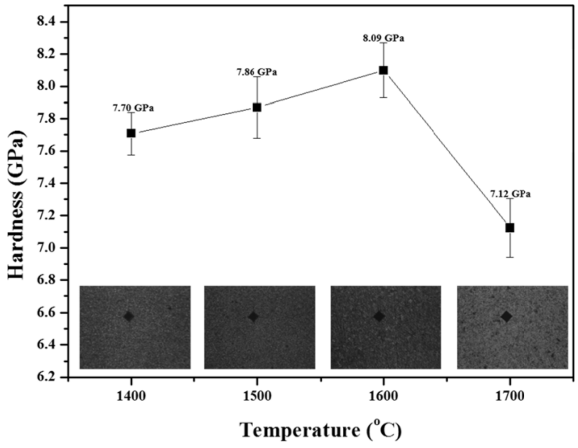

Fig. 6. Effect of SPS temperature on Vickers hardness.

uniform grains. For the specimen sintered at 1600 °C, almost no micropores within grains are observed. As the sintering temperature increases, the growth of the grains is accelerated, thereby decreasing the pores. As seen in Fig. 2, no pores are present in the specimen sintered at 1600 ºC and it has a dense, uniform microstructure. Such dense structures exhibit a higher transmittance [9]. In contrast, intergranular pores are present in the specimen sintered at 1700 ºC owing to the failure in controlling the rapid grain growth and grain densification caused by the rapid temperature increase.

Fig. 4 illustrates the photograph of a specimen subjected to sintering using SPS and annealing in oxygen atmosphere. As compared with the image shown in Fig. 1, the as-annealed specimens exhibit a higher transparency as compared to the as-sintered specimens. The samples sintered at 1600 ºC and annealed exhibit a particularly higher degree of transparency.

Fig. 5 shows the transmittance spectrum of the sintered Y_2O_3 specimen obtained before and after annealing. The results are inconsistent with those obtained by visual examination (Figs. 1 and 4) and sintering density measurements (shown in Fig. 2). With an increase in the sintering temperatures, the transmittance of the samples in the entire wavelength region increases. The specimens annealed in oxygen atmosphere exhibit a higher transmittance as compared to the as-sintered specimens. This could be attributed to the re-diffusion of oxygen inside the sintered Y_2O_3 ceramics as well as the removal of remaining carbon and elimination of oxygen vacancy [10]. Accordingly, the issues such as

Table 1. In-line transmittance of the fabricated transparent Y_2O_3 ceramics by spark plasma sintering.

	Wavelength (nm)	1400 °C	1500 °C	1600 °C	1700 °C
As-sintered	700 nm	22.09%	26.96%	45.15%	38.42%
	1000 nm	30.64%	37.85%	58.55%	52.13%
	1500 nm	42.61%	52.58%	69.20%	65.70%
	2000 nm	52.93%	60.36%	73.30%	73.01%
After-annealed	700 nm	47.49%	53.41%	63.44%	53.45%
	1000 nm	56.20%	65.13%	70.07%	58.17%
	1500 nm	66.85%	74.50%	76.38%	66.29%
	2000 nm	75.19%	80.03%	82.15%	71.00%

Table 2. In-line transmittance at the wavelength of 1000 nm for transparent Y_2O_3 fabricated by different methods.

Method	Sintering condition	Thickness	Transmittance	Ref.
Pressureless Sintering	Step 1: Powders preparation Step 2: 1450 °C, 0 hr, air Step 3: 900 °C, 20 hrs, air Step 4: 1700 °C, 4 hrs, vacuum	1.8 mm	78%	[14]
Pressureless Sintering plus HIP	Step 1: Powders preparation Step 2: 1500 °C, 0 hr, vacuum Step 3: 1400 °C, 20 hrs, vacuum Step 4: 1400 °C, 3 hrs, Ar, HIP, 206 MPa	not given	75%	[15]
	Step 1: Cold pressed, 632 MPa, 30 min Step 2: 1600 °C, 2 hrs, air Step 3: 1650 °C, 6 hrs, Ar, HIP, 203 MPa	0.5 mm	62%	[19]
	Step 1: Cold isostatic pressing, 200 MPa Step 2: 1600 °C, 3 hrs, vacuum Step 3: 1500 °C, 3 hrs, vacuum, HIP, 200 MPa	1.5 mm	41%	[2]
SPS	Step1 : 1299 °C, 1 hrs, vacuum, 300MPa, heating rate : 17 °C/min	1 mm	76%	[11]
	Step1 : 1050 °C, 1 hr, vacuum, 300MPa, heating rate : 20 °C/min	1 mm	75%	[16]
	Step1 : 1600 °C, 5 min, vacuum, 30MPa, heating rate : 100 °C/min	1 mm	70%	In this work

the oxygen vacancy and carbon presence in the Y_2O_3 specimen could be resolved using the annealing process, thereby causing a blue-shift in the ultraviolet absorption edge and improving the transparency of the specimen [11]. Table 1 summarizes the wavelength-specific transmittance of the Y_2O_3 specimens produced by SPS. The rates can be calculated using the Beer-Lambert law. According to the study carried out by Y. Nigara, the theoretical transmittance of the single-crystal Y_2O_3 is 82.6% at 2000 nm [12]. The Y_2O_3 specimen sintered at 1600 °C exhibits a transmittance of 63.44% at λ = 700 nm and 82.15% at 2000 nm. The specimen sintered at 1600 °C exhibits 99% of the theoretical transmittance value in the near infrared region (2000 nm) after annealing. The transmittance obtained at 700 nm in the visible region is also high; however, it is relatively lower than that obtained in the near infrared region. This could be attributed to the effects of micropores owing to the relatively higher levels of scattering being activated when light passes through the ceramic in nanoscale ranges [13].

Table 2 summarizes the transmittance rates (at 1000 nm) of the transparent Y_2O_3 ceramic specimens sintered using various techniques (some of the reported results were not used for comparison because the transmittance values of the transparent Y_2O_3 ceramics were not provided). Lin sintered the Y_2O_3 powder compounds initially to 1450 °C using liquid-based methods followed by performing sintering at 900 °C for 20 hrs and pressureless sintering for 4 hrs at 1700 °C. The obtained transparent Y_2O_3 ceramic exhibited a transmittance of 78% at 1000 nm [14]. Ballato et al. employed a 2-step sintering process at 1500 °C and 1400 °C followed by carrying out HIP sintering for 3 hrs at 1400 °C. The obtained sample exhibited a transmittance of 75% at 1000 nm [15]. Liqiong et al. carried out an SPS-based study by sintering samples for 1 hr at 1299 °C, thereby producing transparent Y_2O_3 ceramics with a transmittance of 76% and density of 99% [11]. Zhang et al. sintered Y_2O_3 ceramic samples for 1 hr at 1050 °C to achieve a density of 99.9% and transmittance of 75% [16]. Thus, all of the studies performed using SPS as a sintering technique (e.g., by Liqiong and Haibin Zhang) resulted in the successful production of transparent Y_2O_3 ceramics exhibiting a high density and transmittance using a single-step process [11, 16]. The diffusion of Y^{3+} across the grain boundary (GB) is considered as the key mechanism for controlling the densification. The diffusion coefficient of Y^{3+} in SPS-based sintering is considerably greater than that achieved

with other sintering techniques [17]. Similarly, Yosida et al. reported a significant improvement in Y_2O_3 GB migration on using SPS [18]. In this work achieved a high transmittance of 70% at 1000 nm and a very high density of 99% with extremely quick SPS followed by annealing.

Fig. 6 shows the Vickers hardness values measured with respect to the sintering temperature. As the SPS temperature increases from 1400°C to 1600°C, the hardness increases from 7.70 GPa to 8.09 GPa. However, the hardness of the sample sintered at 1700 °C decreases to 7.26 GPa owing to the pore growth caused by the rapid grain growth. A similar increase in porosity and decrease in hardness has been previously reported [19-21].

Conclusions

Pure, transparent Y_2O_3 ceramics were easily produced using SPS performed for 5 min at 30 MPa at 1400-1700 °C. The transmittance rate (%) of the 1 mm-thick specimen gradually increased as the sintering temperature increased. A specimen was sintered at 1600 °C and then subjected to annealing for 4 hrs in oxygen atmosphere at 1100 °C. The results indicated an in-line transmittance with a high transmittance of 82.15% at 2000 nm. The optimum sintering conditions for the transparent Y_2O_3 ceramics were found to be 1600 °C, 30 MPa, and 5 min, as the relative density and Vickers hardness values of 98.96% and 8.9 GPa, respectively, could be achieved. The implementation of annealing after SPS carried out at lower temperatures within a short time allowed the production of transparent Y_2O_3 ceramics with a density close to the theoretical density.

Acknowledgments

The authors gratefully acknowledge funding from the AMES Micron Co., LTD., Republic of Korea (2016 00000002413) for financial and support.

Referencs

1. M.S. He, J.B. Li, H. Lin, G.F. Guo and L. Liang, J. Rare earths 24 (2006) 222-224.
2. [J. Mouzona A. Maitre, L. Frisk, N. Lehto and M. Oden, J. Eur. Ceram. Soc. 29 (2009) 311-316.
3. K.H. Kim and K.B. Shim, Mater. Charact. 50 (2003) 31-37.
4. S.H. Shim, J.W. Yoon, K.B. Shim, J. Matsushita, B. S. Hyun and S. G. Kang, J. Alloy. Compd. 413 (2006) 188-192.
5. R. Chaim, R. Marder-Jaeckel and J.Z. Shen, Mater. Sci. Eng. A. 429 (2006) 74-78.
6. M. Tokita, New Ceram. 63 (1997) 1-13.
7. [R.S. Razavi, M.A. Vadeqani, M. Barekat, M. Naderi, S.H. Hashemi and A.K. Mishra, Ceram. Int. 42 (2016) 7819-7823.
8. G. Bernard-Granger, N. Benameur, C. Guizard and M. Nygren, Scripta. Mater. 60 (2009) 164-167.
9. J. Zhang, L. An, M. Liu, S. Shimai and S. Wang J. Eur. Ceram. Soc. 29 (2009) 305-309.
10. B. Ahmadi, S.L. Reza, M. Ahsanzadeh-Vadeqani and M. Barekat, Ceram. Int 42 (2016) 17081-17088.
11. L. An, A. Ito and T. Goto, J. Eur. Ceram. Soc. 32 (2012) 1035-1040.
12. Y. Nigara, Jpn. J. Appl. Phys. 7 (1968) 404-408.
13. K. Ning, J. Wang, D. Luo, J. Ma, J. Zhang, Z.L. Dong and L.B. Kong Opt. Mater 50 (2015) 21-24.
14. Y.H. Huang, D.L. Jiang, J.X. Zhang and Q.L. Lin, J. Am. Cream. Soc. 92 (2009) 2883.
15. K. Serivalsatit, B. Kokuoz, B. Yazgan-Kokuoz, M. Kennedy and J. Ballato, J. Am. Cream. Soc. 93 (2010) 1320.
16. H. Zhang, B.N. Kim, K. Morita, H. Yoshida, K. Hiraga and Y. Sakka, J. Am. Ceram. Soc. 94 (2011) 3206-3210.
17. R. Chaim, A. Shlayer and C. Estournes, J. Eur. Ceram. Soc. 29 (2009) 91-98.
18. H. Yoshida, K. Morita, B.K. Kim, K. Hiraga, K. Yamanaka, K. Soga and T. Yamamoto, J. Am. Ceram. Soc. 94 (2011) 3301-3307.
19. H. Eilers, J. Eur. Ceram. Soc. 27 (2007) 4711–4717.
20. R.W. Rice, J. Mater. Sci. 31 (1996) 1969-1983.
21. F.P. Knudsen, J. Am. Ceram. Soc. 42 (1959) 376-387.
22. R.W. Rice, J. Mater. Sci. 28 (1993) 2187-2190.